



國立台灣大學理學院地質科學系

106 臺北市羅斯福路四段一號

Department of Geosciences, National Taiwan University

No. 1, Sec. 4, Roosevelt Road, Taipei 106, TAIWAN R.O.C.

Tel: +886-2-33662918

Fax: +886-2-33636095

April 10, 2014

Editor of the *Climate of the Past*
Editorial Office
Climate of the Past
European Geosciences Union

Dear Editor:

Enclosed please find an electronic copy of our revised manuscript "Stalagmite-inferred variability of the Asian summer monsoon during the penultimate glacial/interglacial period" by Li *et al.* (CP-2003-170). We would like to submit it as an article to the special issue entitled "Western Pacific paleoceanography - an ocean history perspective on climate variability at orbital to centennial scales". The material in this submission includes: (1) main text, (2) six figures, and (3) one table. None of the material has been published or is under consideration elsewhere, including the internet.

We are pleased by the very positive and constructive nature of the reviews. We have made attempt to incorporate suggestions and the comments of the Editor, Dr. Mahyar Mohtadi. Please see the details of our implementation of the reviews in the attached file "response_to_review_comments-cp-2003-170.pdf". We have incorporated reviewers' suggestions and comments for modifying portions from ABSTRACT to CONCLUSIONS. The manuscript has, thus, been revised throughout.

If this manuscript can be accepted, please consider arranging a good publication time. It will be much appreciated. Please accept our deep appreciation again for your assistance about this submission. We look forward to hearing from you.

Sincerely,

A handwritten signature in black ink, appearing to read 'Chuan-Chou Shen'.

Chuan-Chou Shen

Department of Geosciences, National Taiwan University

No. 1, Sec. 4, Roosevelt Road, Taipei 106, Taiwan ROC.

TEL: 886-2-3366-5878 FAX: 886-2-3365-1917

Email: river@ntu.edu.tw

1 **Stalagmite-inferred variability of the Asian summer monsoon during**
2 **the penultimate glacial/interglacial period**

3
4 **T.-Y. Li^{1,2,3}, C.-C. Shen^{3*}, L.-J. Huang³, X.-Y. Jiang⁴, X.-L. Yang¹, H.-S. Mii⁵,**
5 **S.-Y. Lee⁶, L. Lo³**

6
7 ¹ Key Laboratory of Eco-environments in Three Gorges Reservoir Region, Ministry of
8 Education; School of Geographical Sciences; Southwest University, Chongqing
9 400715, China

10 ² State Key Laboratory of Loess and Quaternary Geology, Institute of Earth
11 Environment, CAS, Xi'an 710075, China

12 ³ High-Precision Mass Spectrometry and Environment Change Laboratory (HISPEC),
13 Department of Geosciences, National Taiwan University, Taipei 10617, Taiwan ROC

14 ⁴ College of Geographical Science; Fujian Normal University, Fuzhou 350007, China

15 ⁵ Department of Earth Sciences, National Taiwan Normal University, Taipei 11677,
16 Taiwan ROC

17 ⁶ Research Center for Environmental Changes, Academia Sinica, Taipei 11529,
18 Taiwan ROC

19
20 April, 10, 2014 revised to *Climate of the Past*:

21 Special issue of **“Western Pacific Paleoceanography - An Ocean History**
22 **Perspective on Climate Variability at Orbital to Centennial Scales”**

23
24 ***Corresponding author:**

25 **C.-C. Shen: National Taiwan University, E-mail: river@ntu.edu.tw**

26 **(Tel) 886-2-3366-5878; (Fax) 886-2-3365-1917.**

27

28 **Abstract**

29 The orbital-timescale dynamics of the Quaternary Asian summer monsoons (ASM)
30 are frequently attributed to precession-dominated northern hemisphere summer
31 insolation. However, this long-term continuous ASM variability is inferred primarily
32 from oxygen isotope records of stalagmites, mainly from Sanbao cave in mainland
33 China, and may not provide a comprehensive picture of ASM evolution. A new
34 spliced stalagmite oxygen isotope record from Yangkou cave tracks summer monsoon
35 precipitation variation from 124-206 thousand years ago in Chongqing, southwest
36 China. Our Yangkou record supports that the evolution of ASM was dominated by the
37 North Hemisphere solar insolation (NHSI) on orbital timescales. When superimposed
38 on the Sanbao record, the Yangkou-inferred precipitation time series supports the
39 strong ASM periods at marine isotope stages (MIS) 6.3, 6.5, and 7.1 and weak ASM
40 intervals at MIS 6.2, 6.4, and 7.0. This consistency confirms that ASM events affected
41 most of mainland China. Except for the solar insolation forcing, the large amplitude
42 of minimum $\delta^{18}\text{O}$ values in Yangkou record during glacial period, such as MIS 6.5,
43 could presumably related to the enhanced prevailing Pacific trade wind and/or
44 continental shelf exposure in the Indo-Pacific warm pool.

45

46

47

48 **Keywords:** Asian summer monsoon, Yangkou cave, stalagmite, glacial/interglacial,

49 Walker Circulation

50 **1 Introduction**

51 Climate in East Asia, the most densely populated region in the world, is
52 profoundly influenced by the Asian monsoon (AM). Asian summer monsoon (ASM)
53 precipitation strongly governs regional vegetation, agriculture, culture, and economies
54 (e.g., Cheng et al., 2012a), and even affected the stability of Chinese dynastic rule
55 (Zhang et al., 2008; Tan et al., 2011). Recent studies have led to significant advances
56 in understanding Quaternary ASM evolution on different time scales (e.g., An, 2000;
57 Wang et al., 2001; 2008; Fleitmann et al., 2003; 2004; Rousseau et al. 2009; Cheng et
58 al., 2009; 2012b; Zhang et al., 2008; Sinha et al., 2011).

59 Our current understanding of ASM variation over past 500 kyr BP (before AD
60 1950) has been reconstructed using oxygen isotope records of Chinese stalagmites
61 (Wang et al., 2008; Cheng et al., 2012b) with the advantages of absolute and
62 high-precision chronologies (e.g., Cheng et al., 2000; 2013; Shen et al., 2002; 2012).
63 Stalagmite-inferred orbital-scale ASM intensity closely follows the change in
64 precession-dominated Northern Hemisphere (NH) summer insolation (NHSI) (Wang
65 et al., 2008; Cheng et al., 2012b). However, these 100s-kyr records were mainly from
66 a single cave, namely Sanbao cave, located in Hubei Province, China (Fig. 1; Wang et
67 al., 2008; Cheng et al., 2012b). Utilizing only one site leads to uncertainties in the
68 spatial extent of Quaternary ASM evolution. These uncertainties stem from
69 differences in local or regional climatic and environmental conditions (Lachniet,
70 2009), hydrological variability of monsoonal sources (e.g., Dayem et al., 2010;
71 Clemens et al., 2010; Pausata et al., 2011), and interactions between climatic
72 subsystems (e.g., Maher and Thompson, 2012; Tan, 2013).

73 Sanbao records, for example, show distinct ASM events at marine isotope stages
74 (MIS) 6.3 and 6.5 during the penultimate glacial time and a weaker summer monsoon

75 during the penultimate glacial maximum (PGM) at MIS 6.2 (Fig. 1 of Wang et al.,
76 2008). To clarify whether this combination of weak PGM ASM intensities and strong
77 ASM events during the penultimate glacial/interglacial (G/IG) period are local effects,
78 we built an integrated stalagmite oxygen stable isotope record from Yangkou cave,
79 Chongqing, China, covering 124-206 kyr BP (Fig. 1). Comparison with records from
80 other Chinese caves (Cheng et al., 2006; 2009; Wang et al., 2008) confirms the
81 fidelity of Sanbao cave-inferred ASM intensities.

82 **2 Material and methods**

83 **2.1 Regional settings and samples**

84 Stalagmites were collected from Yangkou cave (29°02'N, 107°11'E; altitude:
85 2140 m; length: 2245 m), located at Jinfo Mountain National Park, Chongqing City,
86 southwestern China (Fig. 1) during two field trips in 2010 October and 2011 July. The
87 cave, developed in Permian limestone bedrock, is 400 km southwest of Sanbao cave
88 (31°40'N, 110°26'E) in Hubei Province (Wang et al., 2008). The cave air temperature
89 is 7.5 °C and the average relative humidity is >80% (2011 October-2013 October).
90 The regional climate is dominated by the AM and annual rainfall is 1400-1500 mm,
91 83% from April to October (Zhang et al., 1998). Five stalagmites, YK05, YK12,
92 YK23, YK47 and YK61, which formed within a time interval of 124-206 kyr BP were
93 halved and polished for U-Th dating and oxygen stable isotope analysis.

94 **2.2 U-Th dating**

95 Chemistry and instrumental analysis were conducted in the High-Precision Mass
96 Spectrometry and Environment Change Laboratory (HISPEC), Department of
97 Geosciences, National Taiwan University. Fifty three powdered subsamples, 60-80
98 mg each, were drilled from the polished surface along the deposit lamina of the five

99 stalagmites (Fig. 2, Table 1), on a class-100 bench in a class-10,000 subsampling
100 room. U-Th chemistry (Shen et al., 2003) was performed in a class-10,000 clean room
101 with independent class-100 benches and hoods (Shen et al., 2008). A multi-collector
102 inductively coupled plasma mass spectrometer (MC-ICP-MS), Thermo Fisher
103 Neptune, with secondary electron multiplier protocols, was used for the determination
104 of U-Th isotopic contents and compositions (Shen et al., 2012). The decay constants
105 used are $9.1577 \times 10^{-6} \text{ yr}^{-1}$ for ^{230}Th and $2.8263 \times 10^{-6} \text{ yr}^{-1}$ for ^{234}U (Cheng et al.,
106 2000), and $1.55125 \times 10^{-10} \text{ yr}^{-1}$ for ^{238}U (Jaffey et al., 1971). All errors of U-Th
107 isotopic data and U-Th dates are two standard deviations (2σ) unless otherwise noted.
108 Age (before AD 1950) corrections were made using an $^{230}\text{Th}/^{232}\text{Th}$ atomic ratio of $4 \pm$
109 2 ppm, which are the values for material at secular equilibrium, with the crustal
110 $^{232}\text{Th}/^{238}\text{U}$ value of 3.8 (Taylor and McLennan, 1995) and an arbitrary uncertainty of
111 50%

112 **2.3 Stable isotopes**

113 Five-to-seven coeval subsamples, 60-120 μg each, were drilled from one layer
114 per stalagmite to measure the oxygen and carbon isotopic compositions as part of the
115 so-called “Hendy Test” (Hendy, 1971). To obtain oxygen time series, 604 subsamples,
116 60-120 μg each, were drilled at 0.5-3.0 mm intervals along the maximum growth axis.
117 Measurement of oxygen stable isotopes was performed by two isotope ratio mass
118 spectrometers, including a Finnigan Delta V Plus in the Southwest University, China
119 and a Micromass IsoPrime instrument at the National Taiwan Normal University.
120 Oxygen isotope values were reported as $\delta^{18}\text{O}$ (‰) with respect to the Vienna Pee Dee
121 Belemnite standard (V-PDB). An international standard, NBS-19, was used in both
122 laboratories to confirm that the 1-sigma standard deviation of $\delta^{18}\text{O}$ was better than
123 $\pm 0.1\text{‰}$.

124 **3 Results and discussion**

125 **3.1 Chronology**

126 U-Th isotopic and concentration data and dates of all stalagmite subsamples are
127 given in Table 1. High uranium levels range from 0.8-13 ppm and relatively low
128 thorium contents from 100s-10,000 ppt. Corrections for initial ^{230}Th are less than 90
129 yrs, much smaller than dating uncertainties of 400-1,800 yrs that are common for
130 stalagmites with these ^{230}Th ages (Table 1). Determined age intervals are 179.6-189.8,
131 133.7-181.9, 172.6-206.8, 130.0-132.1, and 97.2-172.5 kyr BP for stalagmites YK05,
132 YK12, YK23, YK47, and YK61, respectively (Fig. 3). One to two hiatuses are
133 observed for stalagmites, YK12, YK23, and YK61 (Figs. 2, 3). The chronology of
134 each stalagmite was developed using linear interpolation between U-Th dates, which
135 are all in stratigraphic order (Fig. 3).

136 **3.2 Yangkou oxygen isotope data**

137 The well-known Hendy Test has been taken as an essential requirement when
138 assessing the ability of stalagmites to serve as paleoclimate archives (Hendy, 1971)
139 (Fig. 4). Despite relative large $\delta^{13}\text{C}$ variations of 0.2-0.4‰ (1σ) for coeval
140 subsamples on the five selected layers (Fig. 4A), only a small variations in $\delta^{18}\text{O}$ of
141 ± 0.1 -0.2‰ (1σ) are observed on individual horizons of coeval subsamples (Fig. 4B).
142 Also, there is no relationship between $\delta^{18}\text{O}$ and $\delta^{13}\text{C}$ values, which is an additional
143 part of the Hendy Test (Fig. 4C). The replication of the $\delta^{18}\text{O}$ records both within
144 Yangkou cave (Fig. 5) and between Chinese caves (Fig. 6), as well as successful
145 Hendy Tests, indicates that the stalagmites formed under an oxygen isotopic
146 equilibrium condition. The Yangkou stalagmite $\delta^{18}\text{O}$ data therefore represent rainfall
147 oxygen isotopic change, which is a reflection of regional hydrological variability in

148 the AM territory (e.g., Wang et al., 2001, 2008; Cheng et al., 2009; Li et al., 2011).

149 The oxygen isotope sequences for all of the Yangkou stalagmites are illustrated
150 in Figure 5A. The spliced record covers a time interval from 124-206 kyr BP, with
151 three narrow hiatuses at 132.1-133.5, 190.4-193.2, and 200.3-200.9 kyr BP. This $\delta^{18}\text{O}$
152 record varies from -10‰ to -4‰. The highest $\delta^{18}\text{O}$ data of -5‰ ~ -4‰ occurs at
153 128-136 kyr BP, the PGM.

154 **3.3 Comparison with other Chinese stalagmite records**

155 The new spliced stalagmite $\delta^{18}\text{O}$ sequence from Yangkou cave over the time
156 period of 124-206 kyr BP shows four strong ASM intervals at MIS 5.5, 6.3, 6.5, and
157 7.1 and four weak ASM intervals corresponding to MIS 6.2, MIS 6.4, MIS 7.0, and
158 MIS 7.2 (Fig. 5A). This variation of stalagmite-inferred ASM recorded in Yangkou
159 cave is aligned with previous ASM changes from other Chinese caves, such as Sanbao
160 (Wang et al., 2008; Cheng et al., 2009) and Hulu (32°30'N, 119°10'E) (Cheng et al.,
161 2006), from MIS 5.5-7.2 (Fig. 5).

162 Onsets of strong ASM intervals at MIS 5.5, 6.5, and 7.1 are at 128.3 ± 0.8 , 179.9
163 ± 0.9 , and 201.5 ± 1.1 kyr BP respectively in the Yangkou record and concurrent with
164 their counterparts in Sanbao (Wang et al., 2008; Cheng et al., 2009) and Hulu (Cheng
165 et al., 2006). Transients from strong to weak ASM states occur at 135-136 kyr BP
166 during MIS 6.2-6.3 and 164-165 kyr BP during MIS 6.4-6.5. These also match
167 changes in the Sanbao and Hulu records.

168 Over the past 200 kyr BP, the weakest ASM interval has been suggested to be at
169 MIS 6.2 in the Sanbao records (Wang et al., 2008). For example, the $\delta^{18}\text{O}$ data are 1‰
170 higher than those at weak ASM intervals of MIS 6.4, 7.0, and 7.2 (Fig. 5).
171 Concurrence between ASM records and ice-rafted debris events in the North Atlantic
172 supports the hypothesis of a forcing on the ASM from NH high latitudes (Cheng et al.,

173 2009). $\delta^{18}\text{O}$ values at MIS 6.2 in Yangkou record are 1.5-2‰ higher than those at MIS
174 6.4, 7.0, and 7.2 (Fig. 5). This large difference suggests that this event in Chongqing
175 may have been relatively intensified through NH forcing as compared with the Hubei
176 regions during the PGM.

177 The Sanbao record indicates that the strongest ASM condition over the past 500
178 kyr BP occurs at MIS 6.5 (Cheng et al., 2012b). This ASM event, lasting 13 kyrs, is 3
179 kyrs longer than a comparable event (in terms of intensity) at interglacial MIS 5.3,
180 and was stronger than at any time during MIS 1, 5.5, 7.3, 9.5, and 11.3, which had
181 higher sea-level and NH insolation (Fig. 1 of Cheng et al., 2012b). The lowest
182 contemporaneous $\delta^{18}\text{O}$ data in the Yangkou record (Fig. 5) show a similar ASM
183 intensity at MIS 6.5 in southwest China.

184 During the MIS 5, the variations of Chinese stalagmite $\delta^{18}\text{O}$ records are not
185 consistent among caves (Cheng et al., 2012). In Sanbao record (Wang et al., 2008), a
186 $\delta^{18}\text{O}$ minimum at IMS 5.3 is more depleted than one at MIS 5.5. This phenomenon is
187 seemingly illustrated in Yangkou records (Fig. 5A). However, Dongge (Kelly et al.
188 2006) and Tianmen (Cai et al., 2010a) stalagmite records are characterized by the
189 most depletion in ^{18}O at MIS 5.5 (Fig. 2 of Cai et al., 2010a). This discrepancy may
190 be attributable to different hydrological conditions at MIS 5. Long time series from
191 more Chinese caves are required to derive a clear picture of amplitude changes in
192 relation to orbital forcing at MIS 5.

193 Overall, consistency of the stalagmite $\delta^{18}\text{O}$ sequences between Yangkou and
194 other Chinese caves supports the idea that ASM intensity primarily follows NHSI on
195 orbital timescales and is driven by precessional forcing and is punctuated by NH
196 high-latitude climatic fluctuations (e.g., Wang et al., 2001; 2008; Cheng et al., 2009).
197 Agreement in the amplitude and the transition of $\delta^{18}\text{O}$ dynamics during different MIS
198 also confirms that the Sanbao stalagmite-inferred ASM events at MIS 6, including a
199 very weak one at MIS 6.2 and the strongest one at MIS 6.5, are likely predominant

200 over the entire mainland during the past five G/IG cycles (Cheng et al., 2012a) (Fig.
201 6).

202 **3.4 Forcings for the abnormal strong ASM at MIS 6.5**

203 The extraordinarily strong ASM condition at MIS 6.5 during the penultimate
204 glacial period is one of the most striking features revealed by stalagmite records from
205 three different Chinese caves (Fig. 5). This strong monsoon event is also observed in
206 Chinese Loess plateau record (Rousseau et al., 2009). Modeling experiments suggest
207 this increased monsoon intensity is primarily attributed to high NH insolation
208 (Masson et al., 2000).

209 Wang et al. (2008) found a correlation between the stalagmite-inferred ASM
210 intensity and the atmospheric $\delta^{18}\text{O}$ records from Antarctic Vostok ice core O_2 bubbles
211 (Sowers et al., 1991; Petit et al., 1999), and suggested that the Dole effect (Dole, 1936;
212 Bender et al., 1994) can explain this similarity. A low atmospheric $\delta^{18}\text{O}$ ($\delta^{18}\text{O}_{\text{atm}}$) peak
213 at 170 kyr BP in the Vostok ice core (Petit et al., 1999), for example, matches the
214 strong-ASM period at MIS 6.5.

215 Vostok ice core-inferred $\delta^{18}\text{O}_{\text{atm}}$ evolution most likely results from changes of
216 summer insolation and precipitation in NH, where land provides space for the growth
217 of vegetation and intense photosynthesis during glacial periods (Sun et al., 2000).
218 However, the summer insolation at MIS 6.5 is less than the interglacial periods at MIS
219 5.5 and 7.3 (Fig. 5), suggesting that the minimal stalagmite $\delta^{18}\text{O}$ values at MIS 6.5
220 could also be associated with additional secondary forcing(s).

221 Climate conditions around Yangkou and Sanbao caves are influenced by the
222 Indian summer monsoon (ISM) and East Asian summer monsoon (EASM) (Fig. 1).
223 The ISM, a typical tropical monsoon system, is driven by a south-north land-sea
224 thermal gradient; instead, the EASM is controlled by both south-north and east-west

225 land-sea gradients (Wang and Lin, 2002). The EASM precipitation is influenced by
226 the Northwestern Pacific Tropical High, developed by the mainland-Pacific thermal
227 gradient (Wang et al., 2003). The Pacific climatic variability can, therefore, affect
228 EASM precipitation (Tan, 2013).

229 Cai et al. (2010b) and Jiang et al. (2012) argued for a significant impact of the
230 western tropical Pacific sea surface temperature (SST) on the EASM precipitation.
231 They proposed that the evolution and spatial asynchronicity of stalagmite-inferred
232 Holocene precipitation histories at different AM regions could be attributed to SST
233 changes in the western Pacific. Planktonic foraminiferal-inferred SST records of the
234 marine sediment core ODP806B (0°19'N, 159°22'E) in the western Pacific warm
235 pool (WPWP) and TR163-19 (2°16'N, 90°57'W) in the eastern equatorial Pacific
236 (EEP) (Lea et al., 2000) are plotted in Figure 6, along with the LR04 stacked benthic
237 $\delta^{18}\text{O}$ sequence (Lisiecki and Raymo, 2005) and Yangkou and Sanbao cave time series.
238 A SST gradient between the WPWP and EEP during the glacial periods of MIS 6 and
239 8 is 2 °C, larger than 0.5-1.5 °C gradient during the warm interglacial windows of
240 MIS 5.5 and 7 (Fig. 6). Combined with salinity gradient data, Lea et al. (2000)
241 suggested that the transport of water vapor to the western Pacific was enhanced
242 during glacial times. This large SST gradient could result in an enhanced Walker
243 circulation in the Pacific, similar to the modern La Niña state, which moves the
244 rainfall zone westward and intensifies EASM precipitation (Clement et al., 1999) (Fig.
245 1). Under a weak Walker circulation, analogous to present El Niño conditions, the
246 rainfall zone in the Pacific migrated eastward and EASM precipitation was reduced
247 (Clement et al., 1999). We speculate that the extremely strong EASM precipitation at
248 MIS 6.5 was not only governed by high NHSI, but also partially affected by the
249 Pacific SST gradient.

250 This speculation is supported by modern meteorological observations (e.g, Xue
251 et al., 2007; Tan, 2013) and decadal-resolved marine records (Oppo et al., 2009). La
252 Niña years accompany above-normal precipitation probabilities above normal in
253 mainland China (Tan, 2013 and references therein). Two thousand year-SST and
254 -salinity records from the Makassar Strait (Oppo et al., 2009) also support a strong
255 link between Pacific Ocean climate and the AM. However, comparison of SST
256 histories in the South China Sea and eastern equatorial Pacific SST suggests an El
257 Niño-like condition for the last glacial time (Koutavas et al., 2002), opposite to the
258 findings by Lea et al. (2000). The study by Koutavas et al. (2002) does not support
259 our argument at MIS 6.5.

260 Sea level change could be one of the secondary factors. Marine proxy records
261 and model simulations show that the exposure of the Sunda shelf at the Last Glacial
262 Maximum (LGM) associated with a low sea-level condition can alter regional
263 hydrologic pattern in Southeast Asia (DiNezio and Tierney, 2013). During the LGM,
264 the strong Pacific equatorial SST gradient could strengthen the Pacific Walker
265 circulation and increase rainfall in the west tropical Pacific. While, as pointed out by
266 DiNezio and Tierney (2013), both of the proxies and model simulations are highly
267 uncertain renditions to climate history, multi-proxy records and high precise models
268 are critical to understand paleoclimate.

269 **3.5 Abrupt ASM changes**

270 One of prominent features ASM dynamics is the occurrence of sudden $\delta^{18}\text{O}$
271 shifts at about the midpoint of NHSI change expressed in all Chinese caves over the
272 study time window (Kelly et al. 2006; Cai et al., 2010a; Wang et al., 2008; Cheng et
273 al., 2012a) (Fig. 5). For example, the jumps from weak to strong ASM states lasted
274 <100 yrs from MIS 6.2-5.5 and 500 yrs from MIS 7.2-7.1 (this study; Wang et al.,

275 2008; Cheng et al., 2009). Climate in Hulu Cave is dominated by EASM; instead,
276 Yangkou and Sanbao caves are located in a region influenced by both EASM and
277 ISM. This agreement of local abrupt $\delta^{18}\text{O}$ changes supports the synchronicity of both
278 monsoon sub-system variations on orbital timescale (e.g., Cheng et al., 2012a) and
279 confirms the robustness and regionality of these abrupt transitions in the vast ASM
280 territory. Yangkou records also support the phase lag between ASM and NHSI (Cheng
281 et al., 2009; 2012a). It could be attributed to the influence of millennial-scale abrupt
282 climate change in NH high latitudes (Proter and An, 1995; Sun et al., 2012), which
283 delayed the response of ASM to the rising NHSI (Ziegler et al., 2010; Cheng et al.,
284 2012a).

285 **4 Conclusions**

286 In this study, our new spliced $\delta^{18}\text{O}$ record of five stalagmites from Yangkou cave,
287 Chongqing, exhibits ASM variability over the time period during 124-206 kyr BP. The
288 prominent consistency between the Yangkou and previous Chinese cave $\delta^{18}\text{O}$
289 sequences confirms the duration and intensity of the encompassed ASM events in the
290 entire mainland. Our data supports the hypothesis that the ASM change primarily
291 follows NHSI on a precessional orbital timescale. The weakest ASM condition during
292 low-insolation MIS 6.2 was influenced by meridional forcing originating from the
293 North Atlantic. The strongest ASM intensity at MIS 6.5 over the past 500 kyr BP
294 (Cheng et al., 2012b) was presumably partially related to zonal forcing and/or sea
295 level change associated with G/IG dynamics of Walker circulation in the Pacific.
296 More robust geological archives and model simulations are needed to decipher
297 detailed mechanism and forcings for G/IG ASM evolution.

298 **Acknowledgements**

299 We thank J. W. Partin of the Institute for Geophysics, University of
300 Texas-Austin, and G. S. Burr of the Department of Physics, University of Arizona, for
301 their constructive comments. This work was supported by the Taiwan ROC MOST
302 and NTU grants (101-2116-M-002-009, 102-2116-M-002-016 and 101R7625 to CCS).
303 This study was also supported by grants under the National Natural Science
304 Foundation of China (NSFC) (41030103 and 41172165 to TYL, 41072141 and
305 41272192 to XLY), the Fundamental Research Funds for the Central Universities
306 (XDJK2013A012 to TYL), and the Opening fund of the State Key Laboratory of
307 Loess and Quaternary Geology (SKLLQG1310 to TYL).
308

309 **References**

- 310 An, Z.: The history and variability of the East Asian paleomonsoon climate,
311 *Quaternary Sci. Rev.*, 19, 171-187, 2000.
- 312 Bender, M., Sowers, T., and Labeyrie, L.: The Dole Effect and its variations during
313 the last 130,000 years as measured in the Vostok ice core, *Global Biogeochem.*
314 *Cycles*, 8, 363-376, 1994.
- 315 Cai, Y. J., Cheng, H., An, Z., Edwards, R. L., Wang, X., Tan, L., and Wang, J.: Large
316 variations of oxygen isotopes in precipitation over south-central Tibet during
317 Marine Isotope Stage 5, *Geology*, 38, 243-246, 2010a.
- 318 Cai, Y. J., Tan, L., Cheng, H., An, Z., Edwards, R. L., Kelly, M. J., Kong, X., and
319 Wang, X.: The variation of summer monsoon precipitation in central China since
320 the last deglaciation, *Earth Planet. Sci. Lett.*, 291, 21-31, 2010b.
- 321 Cheng, H., Edwards, R. L., Hoff, J., Gallup, C. D., Richards, D. A., and Asmerson,
322 Y.: The half-lives of uranium-234 and thorium-230, *Chem. Geol.*, 169, 17-33,
323 2000.
- 324 Cheng, H., Edwards, R. L., Wang, Y., Kong, X., Ming, Y., Kelly, M. J., Wang, X.,
325 Gallup, C. D., and Liu, W.: A penultimate glacial monsoon record from Hulu
326 Cave and two-phase glacial terminations, *Geology*, 34, 217-220, 2006.
- 327 Cheng, H., Edwards, R. L., Broecker, W. S., Denton, G. H., Kong, X., Wang, Y.,
328 Zhang, R., and Wang, X.: Ice Age Terminations, *Science*, 326, 248-252, 2009.
- 329 Cheng, H., Sinha, A., Wang, X., Cruz, F. W., and Edwards, R. L.: The global
330 paleomonsoon as seen through speleothem records from Asia to the Americas,
331 *Clim. Dynam.*, 39, 1045-1062, 2012a.
- 332 Cheng, H., Zhang, P., Spötl, C., Edwards, R. L., Cai, Y., Zhang, D., Sang, W., Tan, M.,
333 and An, Z.: The climatic cyclicity in semiarid-arid central Asia over the past

334 500,000 years, *Geophys. Res. Lett.*, 39, L01705, 2012b.

335 Cheng, H., Edwards, R. L., Shen, C.-C., Polyak, V. J., Asmerom, Y., Woodhead, J.,
336 Hellstrom, J., Wang, Y., Kong, X., and Spötl C.: Improvements in ^{230}Th dating,
337 ^{230}Th and ^{234}U half-life values, and U-Th isotopic measurements by
338 multi-collector inductively coupled plasma mass spectroscopy, *Earth Planet. Sci.*
339 *Lett.*, 371-372, 82-91, 2013.

340 Clemens, S. C., Prell, W. L., and Sun Y.: Orbital-scale timing and mechanisms driving
341 Late Pleistocene Indo-Asian summer monsoons: reinterpreting cave speleothem
342 $\delta^{18}\text{O}$, *Paleoceanography*, 25, PA4207, doi:10.1029/2010PA001926, 2010.

343 Clement, A. C., Seager, R., and Cane, M. A.: Orbital controls on the El Niño/Southern
344 Oscillation and the tropical climate, *Paleoceanography*, 14, 441-456, 1999.

345 Dayem, K. E., Molnar, P., Battisti, D. S., and Roe, G. H.: Lessons learned from
346 oxygen isotopes in modern precipitation applied to interpretation of speleothem
347 records of paleoclimate from eastern Asia, *Earth Planet. Sci. Lett.*, 295, 219-230,
348 2010.

349 DiNezio, P. N., & Tierney, J. E.: The effect of sea level on glacial Indo-Pacific climate,
350 *Nature Geosc.*, 6(6), 485-491, 2013.

351 Dole, M.: The relative atomic weight of oxygen in water and in air a discussion of the
352 atmospheric distribution of the oxygen isotopes and of the chemical standard of
353 atomic weights, *J. Chem. Phys.*, 4, 268-275, 1936.

354 Fleitmann, D., Burns, S. J., Neff, U., Mangini, A., and Matter, A.: Changing moisture
355 sources over the last 330,000 years in northern Oman from fluid-inclusion
356 evidence in speleothems, *Quaternary Res.*, 60, 223-232, 2003.

357 Fleitmann, D., Burns, S. J., Neff, U., Mudelsee, M., Mangini, A., and Matter, A.:
358 Palaeoclimatic interpretation of high-resolution oxygen isotope profiles derived

359 from annually laminated speleothems from southern Oman, *Quaternary Sci. Rev.*,
360 23, 935-945, 2004.

361 Hendy, C. H.: The isotopic geochemistry of speleothems. Part 1, the calculation of the
362 effects of different modes of formation on the isotopic composition of
363 speleothems and their applicability as palaeoclimatic indicators, *Geochim.*
364 *Cosmochim. Acta*, 35, 801-824, 1971.

365 Jiang, X., He, Y., Shen, C.-C., Kong, X., Guo, Y., Li, Z., and Chang, Y.-W.:
366 Stalagmite-inferred Holocene precipitation in northern Guizhou Province, China,
367 and asynchronous termination of the climatic optimum in the Asian monsoon
368 territory, *Chin. Sci. Bull.*, 57, 73-79, 2012.

369 Koutavas, A., Lynch-Stieglitz, J., Marchitto, T. M., and Sachs, J. P.: El Niño-like
370 pattern in ice age tropical Pacific sea surface temperature, *Science*, 297, 226–230,
371 2002.

372 Lachniet, M. S.: Climatic and environmental controls on speleothem oxygen-isotope
373 values, *Quaternary Sci. Rev.*, 28, 412-432, 2009.

374 Lea, D. W., Pak, D. K., and Spero, H. J.: Climate impact of late Quaternary equatorial
375 Pacific sea surface temperature variations, *Science*, 289, 1719-1724, 2000.

376 Li, T.-Y., Shen, C.-C., Li, H.-C., Li, J.-Y., Chiang, H.-W., Song, S.-R., Yuan, D.-X.,
377 Lin, C. D.-J., Gao, P., Zhou, L. P., Wang, J.-L., Ye, M.-Y., Tang, L.-L., and Xie,
378 S.-Y.: Oxygen and carbon isotopic systematics of aragonite speleothems and
379 water in Furong Cave, Chongqing, China, *Geochim. Cosmochim. Acta*, 75,
380 4140-4156, 2011.

381 Lisiecki, L. E., and Raymo, M. E.: A Pliocene-Pleistocene stack of 57 globally
382 distributed benthic $\delta^{18}\text{O}$ records, *Paleoceanography*, 20, PA1003, 2005.

383 Maher, B. A., and Thompson, R.: Oxygen isotopes from Chinese caves: Records not

384 of monsoon rainfall but of circulation regime, *J. Quaternary Sci.*, 27, 615-624,
385 2012.

386 Masson, V., Braconnot, P., Cheddadi, R., Jouzel, J., Marchal, O., and de Noblet, N.:
387 Simulation of intense monsoons under glacial conditions, *Geophys. Res. Lett.*,
388 27, 1747–1750, 2000.

389 Oppo, D. W., Rosenthal, Y., and Linsley, B. K.: 2,000-year-long temperature and
390 hydrology reconstructions from the Indo-Pacific warm pool, *Nature*, 460,
391 1113-1116, 2009.

392 Pausata, F. S. R., Battisti, D. S., Nisancioglu, K. H., and Bitz C. M.: Chinese
393 stalagmite $\delta^{18}\text{O}$ controlled by changes in the Indian monsoon during a simulated
394 Heinrich event, *Nature Geosci.*, 4, 474-480, 2011.

395 Petit, J. R., Jouzel, J., Raynaud, D., Barkov, N. I., Barnola, J.-M., Basile, I., Bender,
396 M., Chappellaz, J., Davis, M., Delaygue, G., Delmotte, M., Kotlyakov, V. M.,
397 Legrand, M., Lipenkov, V. Y., Lorius, G., Pépin, L., Ritz, C., Saltzman, E., and
398 Stievenard, M.: Climate and atmospheric history of the past 420,000 years from
399 the Vostok ice core, Antarctica, *Nature*, 399, 429-436, 1999.

400 Rousseau, D. D., Wu, N., Pei, Y., Li, F.: Three exceptionally strong East-Asian
401 summer monsoon events during glacial times in the past 470 kyr. *Clim. Past*, 5,
402 157-169, 2009.

403 Shen, C.-C., Edwards, R. L., Cheng, H., Dorale, J. A., Thomas, R. B., Moran, S. B.,
404 Weinstein, S. E., and Hirschmann, M.: Uranium and thorium isotopic and
405 concentration measurements by magnetic sector inductively coupled plasma
406 mass spectrometry, *Chem. Geol.*, 185, 165-178, 2002.

407 Shen, C.-C., Cheng, H., Edwards, R. L., Moran, S. B., Edmonds, H. N., Hoff, J. A.,
408 and Thomas, R. B.: Measurement of attogram quantities of ^{231}Pa in dissolved and

409 particulate fractions of seawater by isotope dilution thermal ionization mass
410 spectroscopy, *Anal. Chem.*, 75, 1075-1079, 2003.

411 Shen, C.-C., Li, K.-S., Sieh, K., Natawidjaja, D., Cheng, H., Wang, X., Edwards, R.
412 L., Lam, D. D., Hsieh, Y.-T., Fan, T.-Y., Meltzner, A. J., Taylor, F. W., Quinn, T.
413 M., Chiang, H.-W., and Kilbourne, K. H.: Variation of initial $^{230}\text{Th}/^{232}\text{Th}$ and
414 limits of high precision U-Th dating of shallow-water corals, *Geochim.*
415 *Cosmochim. Acta*, 72, 4201-4223, 2008.

416 Shen, C. -C., Wu, C. -C., Cheng, H., Edwards, R. L., Hsieh, Y. -T., Gallet, S., Chang,
417 C. -C., Li, T. -Y., Lam, D. -D., Kano, A., Hori, M., and Spötl, C.: U-Th isotopic
418 determinations in femtogram quantities and high-precision and high-resolution
419 carbonate ^{230}Th dating by MC-ICP-MS with SEM protocols, *Geochim.*
420 *Cosmochim. Acta*, 99, 71-86, 2012.

421 Sinha, A, Stott, L. D., Berkelhammer, M., Cheng, H., Edwards, R. L., Aldenderfer, M.,
422 Mudelsee, M., and Buckley, B.: A global context for megadroughts in monsoon
423 Asia during the past millennium, *Quaternary Sci. Rev.*, 30, 47-62, 2011.

424 Sowers, T., Bender, M., Raynaud, D., Korotkevich, Y. S., and Orchardo, J.: The $\delta^{18}\text{O}$
425 of atmospheric O_2 from air inclusions in the Vostok ice core: Timing of CO_2 and
426 ice volume changes during the penultimate deglaciation, *Paleoceanography*, 6,
427 679-696, 1991.

428 Sun, X., Li, X., Luo, Y., and Chen, X.: The vegetation and climate at the last
429 glaciation on the emerged continental shelf of the South China Sea, *Palaeogeogr.*
430 *Palaeoclimatol. Palaeoecol.*, 160, 301-316, 2000.

431 Sun, Y., Clemens, S. C., Morrill, C., Lin, X., Wang, X., and An, Z.: Influence of
432 Atlantic meridional overturning circulation on the East Asian winter monsoon,
433 *Nature Geosci.*, 5(1), 46-49, 2012.

434 Tan, L., Cai, Y., An, Z., Edwards, R. L., Cheng, H., Shen, C.-C., and Zhang, H.:
435 Centennial- to decadal-scale monsoon precipitation variability in the semi-humid
436 region, northern China during the last 1860 years: Records from stalagmites in
437 Huangye Cave, Holocene, 21, 287-296, 2011.

438 Tan, M.: Circulation effect: Response of precipitation $\delta^{18}\text{O}$ to the ENSO cycle in
439 monsoon regions of China, *Clim. Dynam.*, doi: 10.1007/s00382-013-1732-x,
440 2013.

441 Taylor, S. R., and McLennan, S. M.: The geochemical evolution of the continental
442 crust. *Rev. Geophys.* 33, 241-265, 1995.

443 Wang, B., and Lin, H.: Rainy season of the Asian-Pacific summer monsoon, *J.*
444 *Climate*, 15, 386-396, 2002.

445 Wang, B., Clemens, S. C., and Liu, P.: Contrasting the Indian and East Asian
446 monsoons: Implications on geologic timescales, *Mar. Geol.*, 201, 5-21, 2003.

447 Wang, Y., Cheng, H., Edwards, R. L., An, Z., Wu, J., Shen, C.-C., and Dorale, J. A.: A
448 high-resolution absolute-dated Late Pleistocene monsoon record from Hulu Cave,
449 China, *Science*, 294, 2345-2348, 2001.

450 Wang, Y., Cheng, H., Edwards, R. L., Kong, X., Shao, X., Chen, S., Wu, J., Jiang, X.,
451 Wang, X., and An, Z.: Millennial- and orbital-scale changes in the East Asian
452 monsoon over the past 224,000 years, *Nature*, 451, 1090-1093, 2008.

453 Xue, J., Zhong, W., and Zhao, Y.: Variations of $\delta^{18}\text{O}$ in precipitation in the Zhujiang
454 (Pearl) river delta and its relationship with ENSO event, *Sci. Geogr. Sin.*, 27,
455 825-830, 2007. (in Chinese with English abstract)

456 Zhang, P., Cheng, H., Edwards, R. L., Chen, F., Wang, Y., Yang, X., Liu, J., Tan, M.,
457 Wang, X., Liu, J., An, C., Dai, Z., Zhou, J., Zhang, D., Jia, J., Jin, L., and
458 Johnson, K. R.: A test of climate, sun, and culture relationships from an

459 1810-Year Chinese cave record, *Science*, 322, 940-942, 2008.

460 Zhang, R., Zhu, X., Han, D., Zhang, Y., and Fang, F.: Preliminary study on karst caves
461 of MT. Jinfo, Nanchuan, Chongqing, *Carsologica Sinica*, 17, 196-211, 1998. (in
462 Chinese with English abstract).

463 Ziegler, M., Tuenter, E., Lourens, L. J.: The precession phase of the boreal summer
464 monsoon as viewed from the eastern Mediterranean (ODP Site 968). *Quaternary*
465 *Sci. Rev.*, 29, 481-1490, 2010.

466

467 **Figure captions**

468 **Fig. 1. (A)** Map of precipitation anomaly (mm/day) in June, July, and August
469 (JJA) of AD 1998-2000 during a La Niña event from July 1998 to 2001 April
470 (http://www.cpc.ncep.noaa.gov/products/analysis_monitoring/ensostuff/ensoyears.shtml)
471 comparing with averaged state of JJA from 1980-2010. Triangle symbols denote
472 cave sites of Yangkou (this study), Sanbao (Wang et al., 2008), and Hulu (Clemens
473 2006). Solid circles indicate marine sediment cores of ODP806B and TR163-19 (Lea
474 et al., 2000). Arrows depict present ground wind directions of the ISM and EASM
475 and also trade wind in the equatorial Pacific. Summer precipitation intensity in eastern
476 and southern China was enhanced during the La Niña event. **(B)** An enlarged map of
477 precipitation anomaly with cave sites of Yangkou, Sanbao, and Hulu.

478 **Fig. 2.** Photographs of the five stalagmites collected from Yangkou cave.
479 Brown dashed curves show hiatuses. Straight lines represent subsampling routes for
480 oxygen isotope measurement. Yellow curves denote drilled subsamples for U-Th
481 dating. White dots are the subsamples collected for Hendy Test (Hendy, 1971).

482 **Fig. 3.** Age models of Yangkou stalagmites, established with U-Th dates with
483 precisions of ± 0.3 -1.0% (horizontal error bars).

484 **Fig. 4.** Hendy Test on the arbitrarily selected laminae of five stalagmites with
485 coeval data of **(A)** $\delta^{13}\text{C}$ and **(B)** $\delta^{18}\text{O}$. **(C)** An absence of relationship between $\delta^{18}\text{O}$
486 and $\delta^{13}\text{C}$ indicates insignificant kinetic fractionation.

487 **Fig. 5.** Cave stalagmite oxygen isotope records of **(A)** Yangkou (this study), **(B)**
488 Sanbao (Wang et al., 2008; Cheng et al., 2009), and **(C)** Hulu (Cheng et al., 2006).
489 U-Th ages and 2-sigma errors were color-coded by stalagmite. Numbers of MIS
490 5.5-7.3 are given by Sanbao record. Gray line is NHSI on 21 July at 30°N.

491 **Fig. 6.** Comparison of Chinese cave $\delta^{18}\text{O}$ records of **(A)** Yangkou and **(B)**
492 Sanbao (Wang et al., 2008; Cheng et al., 2009) with **(C)** reconstructed SST records in
493 the WPWP (core ODP806B) and EEP (core TR163-19) (Lea et al., 2000) and **(D)** a
494 global stack benthic foraminifer $\delta^{18}\text{O}$ sequence LR04 (Lisiecki and Raymo, 2005).
495 Numbers of MIS 5.5-8 are given by LR04 record. Gray line is NHSI on 21 July at
496 30°N. Vertical bars denote high insolation intervals.

Table 1. U-Th isotopic compositions and ^{230}Th ages for subsamples of five Yangkou stalagmites on MC-ICP-MS at the HISPEC, NTU

Subsample ID	Depth (mm)	^{238}U (ppb)	^{232}Th (ppt)	$\delta^{234}\text{U}$ measured ^d	$[\text{}^{230}\text{Th}/\text{}^{238}\text{U}]$ activity ^c	$[\text{}^{230}\text{Th}/\text{}^{232}\text{Th}]$ (ppm) ^d	Age (kyr) uncorrected	Age (kyr, BP) corrected ^{e, e'}	$\delta^{234}\text{U}_{\text{initial}}$ corrected ^b
Stalagmite: YK5									
YK5-01	3.0	8730 ±13	553.0 ±7.1	215.8 ±2.1	1.0192 ±0.0024	265626 ±3445	179,706 ±1325	179,643 ±1325	358.5 ±3.7
YK5-02	24.0	7335 ±14	263.1 ±7.1	218.4 ±2.7	1.0235 ±0.0027	471128 ±12563	180,437 ±1600	180,375 ±1600	363.6 ±4.8
YK5-03	57.0	4322.4 ±7.6	5997 ±17	192.9 ±2.3	1.0002 ±0.0024	11903 ±39	181,192 ±1438	181,102 ±1438	321.9 ±4.1
YK5-04	79.0	5041 ±10	500.2 ±5.7	187.7 ±2.9	0.9997 ±0.0026	166348 ±1928	183,234 ±1713	183,171 ±1713	315.1 ±5.0
YK5-05	88.0	5729.6 ±9.4	356.1 ±5.1	184.6 ±2.4	0.9986 ±0.0027	265267 ±3814	184,166 ±1611	184,103 ±1611	310.6 ±4.2
YK5-06	103.0	5375.3 ±9.9	593.2 ±5.0	202.1 ±2.6	1.0161 ±0.0022	152028 ±1290	184,207 ±1499	184,143 ±1499	340.1 ±4.7
YK5-07	128.0	4986.2 ±8.8	137.6 ±5.8	201.6 ±2.3	1.0175 ±0.0023	608876 ±25827	185,061 ±1436	184,999 ±1436	340.0 ±4.1
YK5-08	149.0	6076 ±14	269.0 ±5.2	205.0 ±3.0	1.0259 ±0.0028	382639 ±7471	187,222 ±1841	187,159 ±1841	348.1 ±5.3
YK5-09	177.0	8808 ±11	1103.7 ±7.2	215.0 ±1.9	1.0374 ±0.0016	136699 ±889	187,890 ±1128	187,826 ±1128	365.7 ±3.5
YK5-10	188.0	12100 ±19	168.3 ±6.1	210.0 ±2.5	1.0368 ±0.0027	1230671 ±44610	189,876 ±1694	189,815 ±1694	359.2 ±4.7
Stalagmite: YK12									
YK12-01	3.6	6262.6 ±4.1	3895 ±24	309.6 ±1.2	0.9620 ±0.0015	25540 ±164	133,762 ±462	133,690 ±462	451.8 ±1.9
YK12-02	10.5	5016.7 ±2.5	12393 ±25	296.1 ±1.2	0.9590 ±0.0017	6410 ±17	135,884 ±510	135,777 ±511	434.7 ±1.8
YK12-03	21.5	6384.1 ±3.6	1050 ±21	296.2 ±1.1	0.9796 ±0.0014	98334 ±1947	141,426 ±463	141,362 ±463	441.8 ±1.7
YK12-04	40.0	5675.3 ±5.8	9675 ±32	273.0 ±1.6	0.9792 ±0.0017	9483 ±34	147,071 ±670	146,978 ±670	413.7 ±2.6
YK12-05	57.5	13314 ±13	1488 ±21	259.4 ±1.5	0.9840 ±0.0015	145382 ±2094	152,201 ±622	152,138 ±622	398.9 ±2.4
YK12-06	78.0	11746.6 ±5.5	1425 ±24	253.54 ±0.90	0.9852 ±0.0013	134061 ±2272	154,298 ±485	154,235 ±485	392.1 ±1.5
YK12-07	80.0	8830.3 ±5.3	38573 ±98	212.8 ±1.2	0.9796 ±0.0027	3702 ±14	165,267 ±1071	165,120 ±1071	339.4 ±2.2
YK12-08	92.0	7106.6 ±3.6	7546 ±25	199.70 ±0.89	0.9823 ±0.0014	15274 ±55	171,076 ±643	170,993 ±643	323.9 ±1.5
YK12-09	101.0	9513.1 ±6.5	4483 ±23	203.4 ±1.1	0.9976 ±0.0013	34954 ±182	175,795 ±717	175,725 ±717	334.3 ±2.0
YK12-10	105.0	5118.6 ±6.7	2378 ±21	185.4 ±1.9	0.9924 ±0.0018	35265 ±317	181,021 ±1132	180,949 ±1132	309.3 ±3.3
YK12-11	109.5	6109.1 ±3.8	572 ±18	178.4 ±1.2	0.9875 ±0.0013	174125 ±5633	181,929 ±770	181,866 ±770	298.4 ±2.1
Stalagmite: YK23									
YK23-01	2.4	2893.2 ±2.3	13899 ±26	102.8 ±1.5	0.8935 ±0.0018	3070.9 ±8.0	172,790 ±1035	172,620 ±1035	167.6 ±2.4
YK23-02	9.6	2608.9 ±1.7	13210 ±23	99.6 ±1.1	0.9008 ±0.0016	2937.3 ±7.1	177,700 ±946	177,525 ±947	164.5 ±1.9
Hiatus									
YK23-03	11.2	2705.2 ±1.3	1370 ±17	59.55 ±0.91	0.8799 ±0.0016	28683 ±355	187,327 ±1030	187,254 ±1030	101.1 ±1.6
YK23-04	14.8	2541.1 ±1.2	10313 ±20	60.06 ±0.89	0.8830 ±0.0015	3592.3 ±8.9	188,729 ±982	188,571 ±982	102.4 ±1.5
Hiatus									
YK23-05	16.8	3255.5 ±2.0	1365 ±14	32.5 ±1.1	0.8632 ±0.0012	33986 ±363	193,472 ±994	193,401 ±994	56.1 ±1.8
YK23-06	27.6	3084.7 ±1.5	2354 ±14	32.53 ±0.92	0.8671 ±0.0012	18764 ±112	195,871 ±932	195,791 ±932	56.6 ±1.6
YK23-07	35.6	2208.7 ±1.3	2343 ±15	47.1 ±1.0	0.8848 ±0.0014	13768 ±89	197,538 ±1069	197,451 ±1069	82.2 ±1.8
YK23-08	42.4	1917.04 ±0.90	4503 ±17	39.3 ±1.1	0.8795 ±0.0013	6182 ±25	199,294 ±1103	199,175 ±1103	68.9 ±1.9
Hiatus									
YK23-09	43.0	2720.4 ±1.5	1128 ±14	21.23 ±0.90	0.8633 ±0.0013	34369 ±430	200,953 ±1095	200,882 ±1095	37.5 ±1.7
YK23-10	62.4	3355.3 ±2.2	698 ±23	16.2 ±1.0	0.8657 ±0.0014	68753 ±2263	206,207 ±1217	206,141 ±1217	29.0 ±1.8
YK23-11	77.2	2262.6 ±1.5	899 ±19	15.0 ±1.1	0.8655 ±0.0015	35976 ±777	206,922 ±1340	206,839 ±1340	26.9 ±2.1
Stalagmite: YK47									
YK47-01	118.8	812.37 ±0.81	6437 ±11	395.2 ±1.8	1.0173 ±0.0022	2120.0 ±6.0	130,186 ±610	129,991 ±612	570.7 ±2.8
YK47-02	137.5	765.96 ±0.70	2997.5 ±7.6	398.9 ±1.8	1.0295 ±0.0019	4343 ±13	132,271 ±565	132,144 ±566	579.7 ±2.8
Stalagmite: YK61									
YK61-01	13.6	3427.4 ±2.1	13736 ±25	295.8 ±1.2	0.9172 ±0.0019	3779 ±10	125,391 ±512	125,255 ±513	421.5 ±1.8
YK61-02	15.5	3636.8 ±1.9	4502 ±12	275.4 ±1.2	0.9027 ±0.0013	12039 ±37	125,800 ±410	125,715 ±411	393.0 ±1.8
YK61-03	17.0	3974.8 ±2.4	4663 ±10	261.5 ±1.2	0.8936 ±0.0013	12577 ±32	126,291 ±408	126,207 ±408	373.6 ±1.8
YK61-04	20.0	3418.6 ±3.7	1271.0 ±8.9	302.6 ±1.8	0.9278 ±0.0013	41205 ±291	126,643 ±476	126,575 ±476	432.9 ±2.6
YK61-05	22.4	1520.4 ±2.4	3627 ±33	340.2 ±2.4	0.9619 ±0.0024	6658 ±63	127,602 ±716	127,496 ±716	487.8 ±3.5
YK61-06	26.0	2414.5 ±4.3	2217 ±29	315.2 ±2.4	0.9448 ±0.0027	16993 ±229	128,330 ±800	128,250 ±800	453.0 ±3.6
YK61-07	28.3	4454.4 ±4.8	801.0 ±8.8	313.7 ±1.7	0.9452 ±0.0013	86784 ±959	128,698 ±470	128,633 ±470	451.4 ±2.5
YK61-08	30.1	2434.4 ±2.3	657.4 ±8.6	314.5 ±1.6	0.9479 ±0.0012	57958 ±756	129,213 ±431	129,146 ±431	453.1 ±2.3
YK61-09	40.8	3633.5 ±4.6	207 ±25	302.5 ±2.1	0.9389 ±0.0019	271567 ±32442	129,373 ±635	129,309 ±635	436.1 ±3.2
YK61-10	47.8	3140.5 ±3.0	132.3 ±7.0	305.6 ±1.6	0.9459 ±0.0013	370865 ±19563	130,518 ±452	130,455 ±452	441.9 ±2.3
YK61-11	61.3	5420.5 ±6.6	3648 ±10	306.2 ±1.8	0.9502 ±0.0016	23311 ±67	131,466 ±546	131,393 ±546	443.9 ±2.7
Hiatus									
YK61-12	63.1	2307.3 ±1.8	1947.5 ±8.3	303.9 ±1.3	0.9801 ±0.0012	19171 ±84	139,776 ±445	139,699 ±445	451.0 ±2.0
YK61-13	74.0	5853.2 ±7.4	3435 ±11	287.2 ±1.7	0.9743 ±0.0017	27409 ±90	142,087 ±626	142,014 ±626	429.2 ±2.7
YK61-14	88.0	3614.8 ±7.1	352 ±20	321.2 ±2.9	1.0365 ±0.0027	175586 ±9727	151,405 ±1087	151,340 ±1087	492.7 ±4.7
YK61-15	110.0	4705.3 ±8.5	672 ±16	320.3 ±2.6	1.0476 ±0.0026	121199 ±2976	154,945 ±1061	154,880 ±1061	496.2 ±4.4
YK61-16	130.0	5173.2 ±8.0	646 ±18	303.7 ±2.3	1.0495 ±0.0022	138661 ±3763	160,250 ±982	160,184 ±982	477.6 ±3.8
YK61-17	137.8	6174.8 ±8.5	405.3 ±7.9	299.4 ±2.0	1.0514 ±0.0019	264459 ±5140	162,165 ±869	162,102 ±869	473.5 ±3.4
YK61-18	167.8	4766.3 ±5.3	347.8 ±7.3	274.1 ±1.7	1.0478 ±0.0014	237115 ±4998	169,056 ±774	168,993 ±774	441.9 ±3.0
YK61-19	185.8	2984.1 ±2.9	1897.4 ±9.4	239.0 ±1.7	1.0238 ±0.0015	26585 ±135	172,561 ±837	172,487 ±837	389.2 ±2.9

Chemistry was performed during 2011-2012 (Shen et al., 2003) and instrumental analyses on MC-ICP-MS (Shen et al., 2012).

Analytical errors are 2σ of the mean.

^a $\delta^{234}\text{U} = ([\text{}^{234}\text{U}/\text{}^{238}\text{U}]_{\text{activity}} - 1) \times 1000$.

^b $\delta^{234}\text{U}_{\text{initial}}$ corrected was calculated based on ^{230}Th age (T), i.e., $\delta^{234}\text{U}_{\text{initial}} = \delta^{234}\text{U} \times e^{\lambda^{234}\text{U} \times T}$, and T is corrected age.

^c $[\text{}^{230}\text{Th}/\text{}^{238}\text{U}]_{\text{activity}} = 1 - e^{-\lambda^{230}\text{Th} T} + (\delta^{234}\text{U}/1000)[\lambda_{230}/(\lambda_{230} - \lambda_{234})](1 - e^{-(\lambda_{230} - \lambda_{234}) T})$, where T is the age.

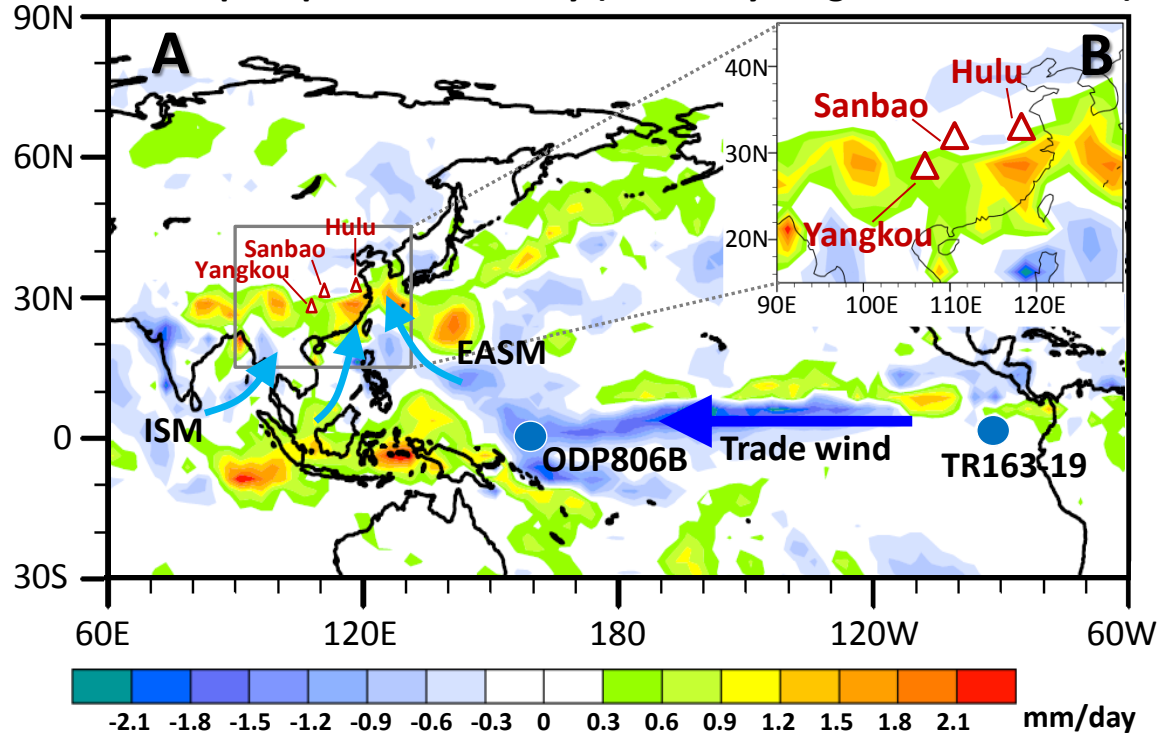
Decay constants used are available in Cheng et al. (2000).

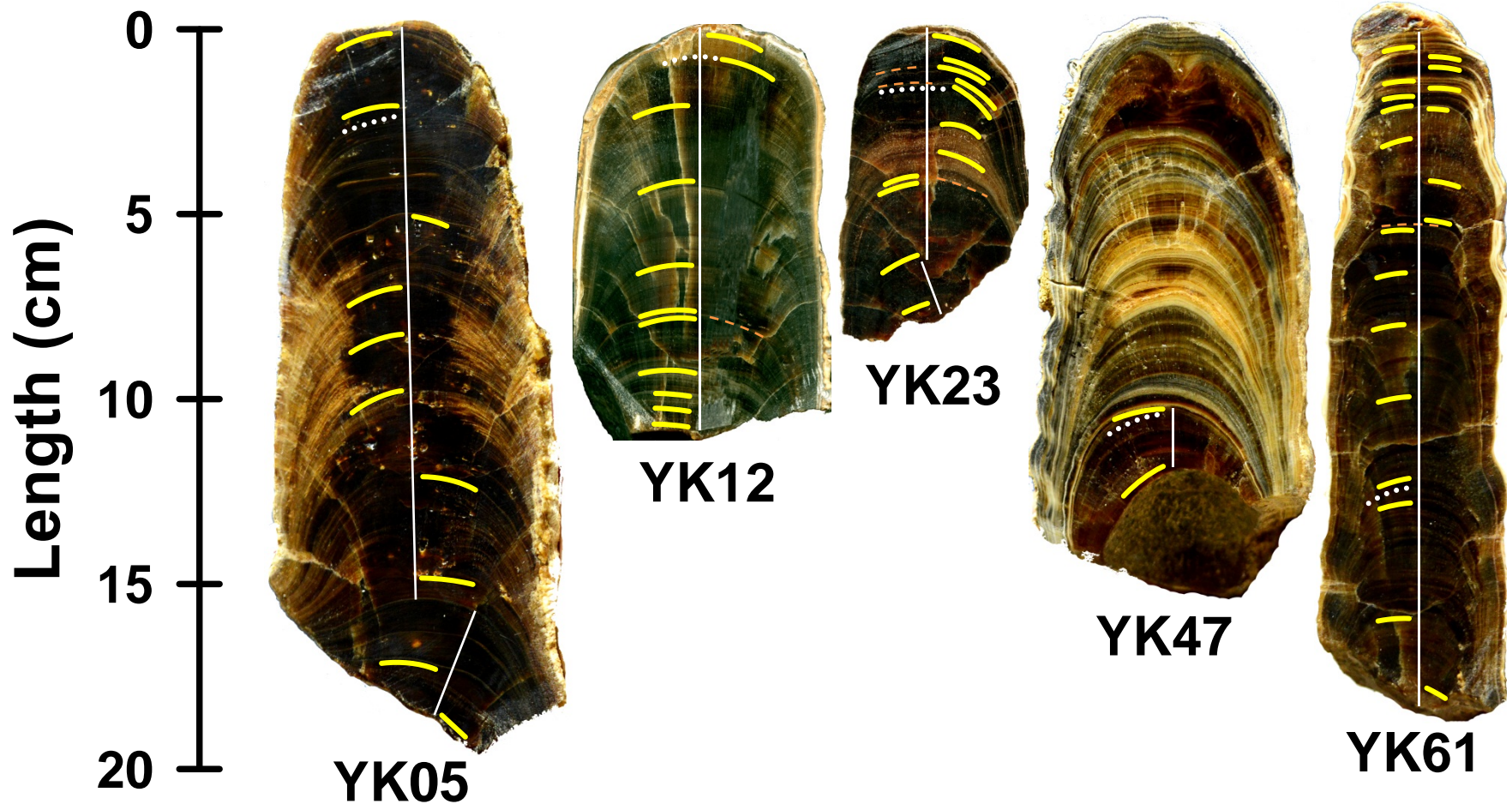
^d The degree of detrital ^{230}Th contamination is indicated by the $[\text{}^{230}\text{Th}/\text{}^{232}\text{Th}]$ atomic ratio instead of the activity ratio.

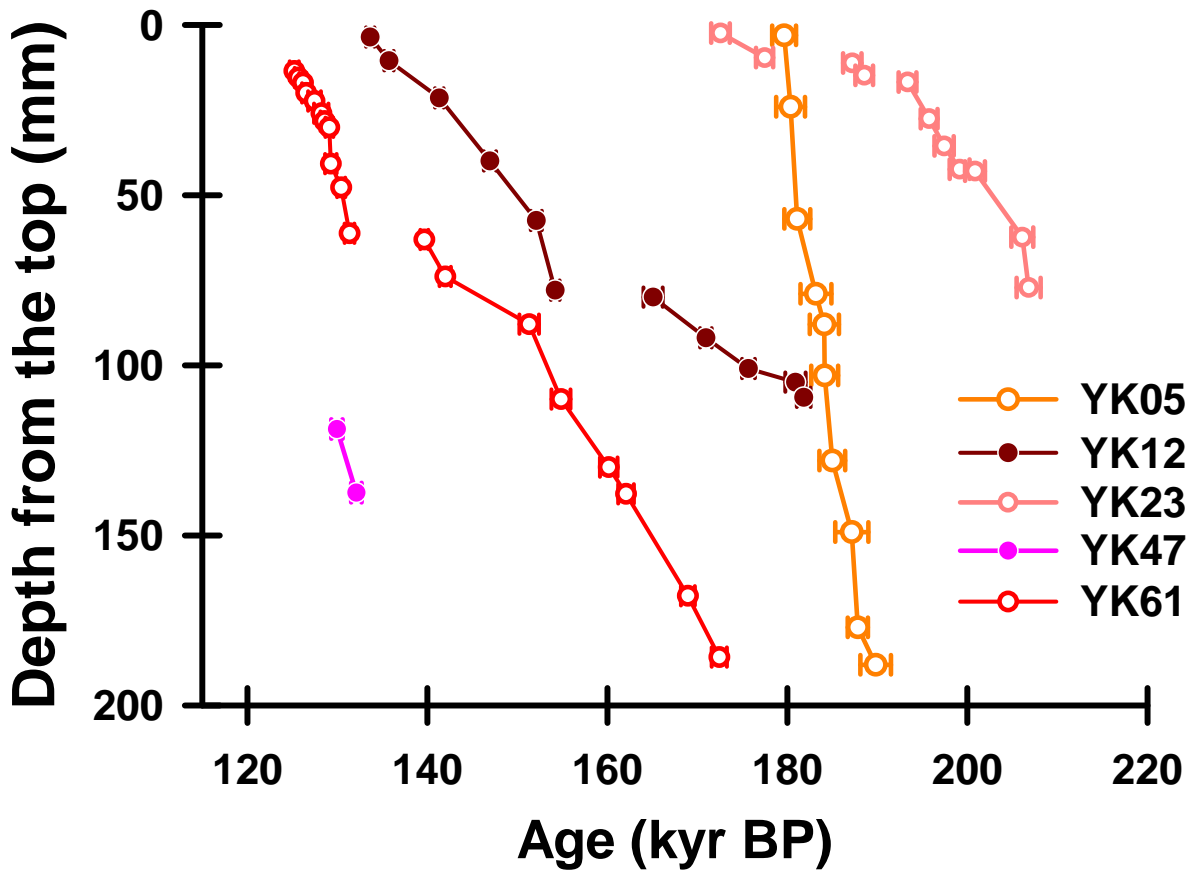
^e Age [yr BP (before AD 1950)] corrections were made using an $^{230}\text{Th}/\text{}^{232}\text{Th}$ atomic ratio of 4 ± 2 ppm.

Those are the values for material at secular equilibrium, with the crustal $^{232}\text{Th}/\text{}^{238}\text{U}$ value of 3.8. The errors are arbitrarily assumed to be 50%.

La Niña precipitation anomaly (June, July, August of 1998-2000)

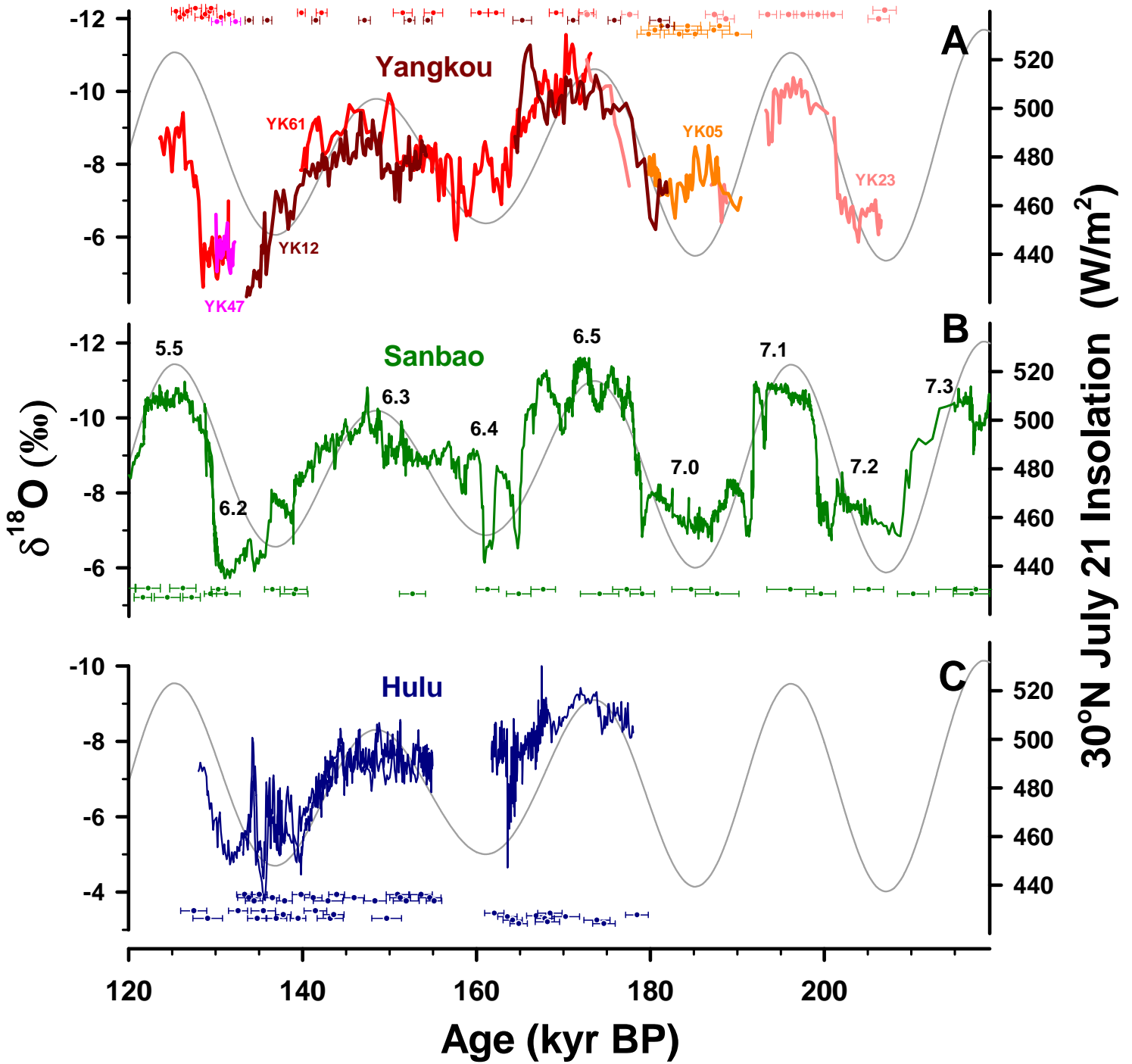


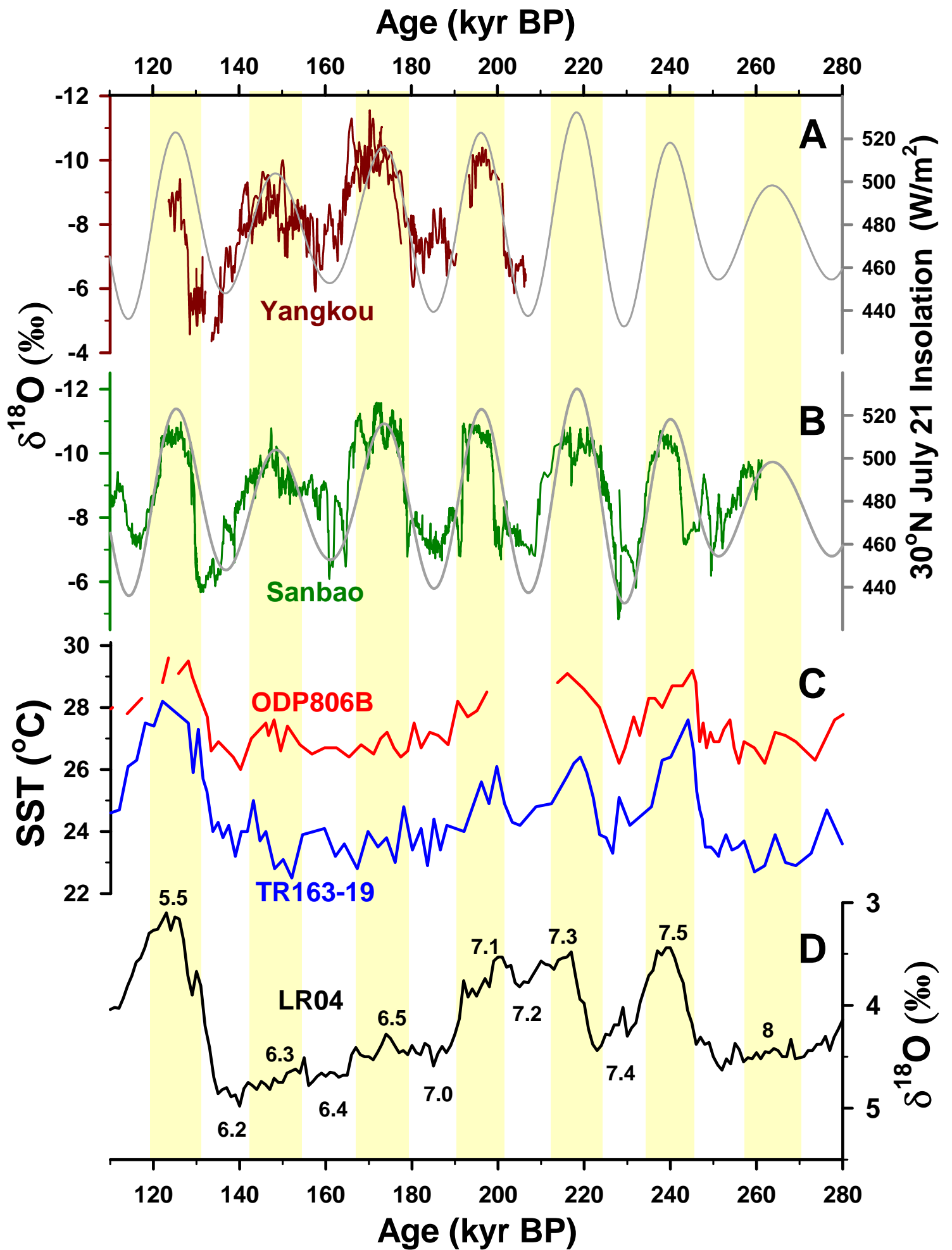




Age (kyr BP)

120 140 160 180 200





We are pleased by the very positive and constructive reviews. We have made every attempt to incorporate the comments/arguments. We believe that we have addressed all reviewers' comments. Please see the details of our implementation of the reviews below.

Points raised by reviewers and editor are shown in blue, Arial type, while our responses are shown in black, Times New Roman type.

Editor: Dr. Mahyar Mohtadi

E1 "First and foremost my apologies regarding the long delay of the review process. We had a large (double-digit) number of declined review invitations, possibly because of the timing of your submission right before the Christmas. When revising your manuscript, please address all the referees' comments in full and send a point-by-point response to their comments. I agree with both referees suggesting to remove the rather speculative discussion of the stalagmite $\delta^{18}\text{O}$ forcing by tropical Pacific SST gradient, unless you find more convincing evidence for this hypothesis. Please also consider that your revised manuscript could be sent to the same referees for further advice, particularly in light of the referee #2 suggestions of expanding certain parts of the discussion on the expense of the others. Hope you find these comments helpful."

Thank Dr. Mohtadi for handing with our case and summarizing issues raised by the reviewers. We have addressed all points, including comments, questions, and suggestions given by reviewers. Please consider our revised manuscript if this version can be accepted by your journal.

Reviewer #1: anonymous

We would like to thank this reviewer for reviewing our manuscript, giving us very valuable suggestions and comments. He said “**General comments:** The manuscript by Li et al. presents a stalagmite oxygen isotope ($\delta^{18}\text{O}$) record from Yangkou Cave, Chongqing, Southwestern China, to infer Asian summer monsoon (ASM) variability during the penultimate glacial/interglacial period. With high-precision ^{230}Th dating, the authors have found that the Asian summer monsoon variability was dominated by strong precessional cycles, consistent with previous stalagmite results from Sanbao and thus suggesting that the stalagmite records indicate a large-scale phenomenon. The authors further suggest that the ASM intensity was strongest at MIS 6.5 during the penultimate glacial period. The authors then compared their records with marine SST and salinity records from the tropical Pacific and suggest that larger zonal SST gradient, and thus intensified Walker Circulation (a La Nina-like state), would have contributed to the stronger ASM intensity at MIS 6.5. I believe that it is an excellent contribution to CPD and recommend its publication.”

Thank this reviewer for recommending publishing. We believed that we have addressed all points raised. Our response is shown in the following section of **R1.1 specific comments**.

R1.1: Specific comments:

The authors specifically picked MIS 6.5 as an example to illustrate the role of tropical Pacific thermal state in affecting the ASM intensity. However, it appears to me that the ASM intensity at MIS 6.5 is largely comparable to other periods such as MIS 6.3, 5.5, and 7.1 (MIS 7.3 and 7.5 as well as inferred from the Sanbao record). If the tropical Pacific thermal state (zonal SST gradient) were so important at orbital timescales, based on the authors' reasoning, much weaker ASM intensity would have occurred at MIS 5.5, 7.1 and 7.3. However, the stalagmite records do not support this argument. Thus, in my opinion, the ASM variability at orbital timescales, as inferred from stalagmite records, is largely independent of the thermal state of tropical Pacific. Why this is the case is still a

mystery to most of us. However, the stalagmite records suggest that the $\delta^{18}\text{O}$ signal is dominantly controlled by the northern hemisphere summer insolation. The thermal state of tropical Pacific, if there is any role at orbital timescales, would be at most secondary.

We thank this reviewer for giving the comments. We agree with the reviewer's comments. The NH summer insolation dominantly controlled the evolution of ASM at orbital timescales all through the late Quaternary epoch. The tropical Pacific thermal state (zonal SST gradient) could be one of possible secondary factors. Reviewer #2 also pointed out this issue more detailed about possible monsoonal forcings at MIS 6.5. We accepted the suggestions of both reviewers and revised all related sections from ABSTRACT to CONCLUSIONS. Please refer to the sections of **R2.2-R2.5** in the reply for reviewer #2 shown below.

Reviewer #2: anonymous

We would like to thank this reviewer for reviewing our manuscript, giving us very constructive suggestions and comments. He said “The authors present a new stalagmite $\delta^{18}\text{O}$ record from a cave in Southwest China, which covers one glacial-interglacial cycle from 206 ka to 124 ka. This record is a valuable addition to the growing number of long speleothem records from China. The important contribution of this new record is that it reproduces interesting features of the Sanbao record, like the large amplitude of the precession-related $\delta^{18}\text{O}$ minimum during glacial stage 6.5. In light of recent debates of the origin of the $\delta^{18}\text{O}$ signal in Chinese caves, the reproducibility of the signal over large areas is an important aspect. In my opinion this is therefore a valuable contribution and should be published in *Climate of the Past*. The authors nicely lay out the basis of their study (Hendy test results, age models) and provide clear and informative figures. However, I have some concerns about the discussion and interpretation of the record. In my view the explanation of the strong MIS 6.5 signal is overly confident (see below) and should be tuned down to a possibility.”

Thank this reviewer for recommending publishing. We agree with the suggestion about the possible forcings at MIS 6.5, which was also questioned by reviewer #1. We have tuned down the zonal forcing as one of possibilities. Please refer to the following sections. We believed that we have addressed all points raised. Our responses have been

shown as sections of particular concerns (**R2.1-R2.5**) and additional specific notes (**R2.6-R2.7**).

R2.1: On the other hand, an important contribution of this record is only mentioned but not discussed further, namely the fact that the timing of the sudden jumps in $\delta^{18}\text{O}$ match between the different records, confirming their robustness and regionality. The sudden $\delta^{18}\text{O}$ decreases (increases) consistently occur about halfway during NH summer insolation increases (decreases). I suggest adding a discussion about this robust observation.

Thank this reviewer for giving this valuable suggestion. We accepted the suggestion and add a more section of “**3.5 Abrupt ASM changes**”.

We wrote “**3.5 Abrupt ASM changes:** *One of prominent features ASM dynamics is the occurrence of sudden $\delta^{18}\text{O}$ shifts at about the midpoint of NHSI change expressed in all Chinese caves over the study time window (Kelly et al. 2006; Cai et al., 2010a; Wang et al., 2008; Cheng et al., 2012a) (Fig. 5). For example, the jumps from weak to strong ASM states lasted <100 yrs from MIS 6.2-5.5 and 500 yrs from MIS 7.2-7.1 (this study; Wang et al., 2008; Cheng et al., 2009). Climate in Hulu Cave is dominated by EASM; instead, Yangkou and Sanbao caves are located in a region influenced by both EASM and ISM. This agreement of local abrupt $\delta^{18}\text{O}$ changes supports the synchronicity of both monsoon sub-system variations on orbital timescale (e.g., Cheng et al., 2012a) and confirms the robustness and regionality of these abrupt transitions in the vast ASM territory. Yangkou records also support the phase lag between ASM and NHSI (Cheng et al., 2009; 2012a). It could be attributed to the influence of millennial-scale abrupt climate change in NH high latitudes (Proter and An, 1995; Sun et al., 2012), which delayed the response of ASM to the rising NHSI (Ziegler et al., 2010; Cheng et al., 2012a).*” (**Lines 269-284**)

R 2.2: The suggested explanation for the large amplitude of the MIS 6.5 $\delta^{18}\text{O}$ minimum (i.e., association with stronger tropical Pacific SST gradients and Walker circulation) is highly speculative and should be stated much more carefully (in the abstract, L. 21-23 on Page 6290, and L. 23-25 on page 6296).

Reviewer #1 questioned the same issue. We thank both reviewers for giving the comments. We have much carefully interpreted the large amplitude of the MIS 6.5 $\delta^{18}\text{O}$ minimum.

In ABSTRACT, we revised as “*Except for the solar insolation forcing, the large amplitude of minimum $\delta^{18}\text{O}$ values in Yangkou record during glacial period, such as MIS 6.5, could presumably related to the enhanced prevailing Pacific trade wind and/or continental shelf exposure in the Indo-Pacific warm pool.*” (**Lines 41-44**).

In INTRODUCTION, we revised a sentence of “Comparison with records from other Chinese caves would confirm the fidelity of Sanbao cave-inferred ASM intensities. Our results also demonstrate that a strong Walker circulation in the Pacific could enhance glacial ASM precipitation.” to “*Comparison with records from other Chinese caves (Cheng et al., 2006; 2009; Wang et al., 2008) confirms the fidelity of Sanbao cave-inferred ASM intensities.*” (Lines 79-81).

In the section **3.4 Forcings for the abnormal strong ASM at MIS 6.5**, we revised a sentence of “The extremely strong EASM precipitation at MIS 6.5 was not only governed by high NHSI, but also enhanced by the Pacific SST gradient.” to “*We speculate that the extremely strong EASM precipitation at MIS 6.5 was not only governed by high NHSI, but also partially affected by the Pacific SST gradient.*” (Lines 247-249)

We revised the last paragraph of Section 3.4 of the original manuscript to “*This speculation is supported by modern meteorological observations (e.g. Xue et al., 2007; Tan, 2013) and decadal-resolved marine records (Oppo et al., 2009). La Niña years accompany above-normal precipitation probabilities above normal in mainland China (Tan, 2013 and references therein). Two thousand year-SST and -salinity records from the Makassar Strait (Oppo et al., 2009) also support a strong link between Pacific Ocean climate and the AM. However, comparison of SST histories in the South China Sea and eastern equatorial Pacific SST suggests an El Niño-like condition for the last glacial time (Koutavas et al., 2002), opposite to the findings by Lea et al. (2000). The study by Koutavas et al. (2002) does not support our argument.*” (Lines 250-259)

R2.3: Firstly, from the Chinese stalagmite records it is not at all clear that amplitudes of precession-related $\delta^{18}\text{O}$ minima are larger during glacial times than during interglacials. In the Sanbao record, the amplitude of MIS 6.5 is similar to or slightly smaller than that of MIS 5.3 (an interglacial period). Furthermore, the amplitudes of the $\delta^{18}\text{O}$ minima seem to not always be consistent among different sites in China. The subdued signal for MIS 5.5 in comparison to MIS 5.3 in Sanbao is not observed in Dongge cave (see Fig 5 in Cheng et al 2012). In my opinion, the large amplitude of the MIS 6.5 minimum in the presented record is indeed a very interesting feature, and it is important that it is replicated in 2 caves 400 km apart. The authors could also mention the correspondence to the Loess plateau record of Rousseau et al. (2009) (as highlighted by Cheng et al. 2012). But given the ambiguities outlined above the interpretation should be done much more carefully. It probably needs long time series from multiple Chinese caves to derive a clear picture of amplitude changes in relation to orbital forcing.

Thank this reviewer for giving the valuable suggestions. In the new version, we discussed the inconsistent change of stalagmite records among Chinese cave as: “*During*

the MIS 5, the variations of Chinese stalagmite $\delta^{18}\text{O}$ records are not consistent among caves (Cheng et al., 2012). In Sanbao record (Wang et al., 2008), a $\delta^{18}\text{O}$ minimum at MIS 5.3 is more depleted than one at MIS 5.5. This phenomenon is seemingly illustrated in Yangkou records (Fig. 5A). However, Dongge (Kelly et al. 2006) and Tianmen (Cai et al., 2010a) stalagmite records are characterized by the most depletion in ^{18}O at MIS 5.5 (Fig. 2 of Cai et al., 2010a). This discrepancy may be attributable to different hydrological conditions at MIS 5. Long time series from more Chinese caves are required to derive a clear picture of amplitude changes in relation to orbital forcing at MIS 5.”. (Lines 184-192)

The Loess plateau record was cited as *“This strong monsoon event is also observed in Chinese Loess plateau record (Rousseau et al., 2009). Modeling experiments suggest this increased monsoon intensity is primarily attributed to high NH insolation (Masson et al., 2000).”*. (Lines 205-208)

R2.4: Secondly, the hypothesis that glacial times were associated with more La Niña-like conditions in the tropical Pacific is also highly uncertain. While the SST differences observed by Lea et al. (2000), which the authors refer to, suggest enhanced zonal temperature gradients during glacial times, other studies have inferred the opposite, more El Niño-like conditions, for glacial times (Koutavas et al 2002). Furthermore, the exposure of the Sunda Shelf during glacial times likely had a strong influence on regional circulation patterns (e.g., DiNezio 2009), which is at present largely unconstrained.

Thank this reviewer for the in-depth comments. We wrote *“This speculation is supported by modern meteorological observations (e.g, Xue et al., 2007; Tan, 2013) and decadal-resolved marine records (Oppo et al., 2009). La Niña years accompany above-normal precipitation probabilities above normal in mainland China (Tan, 2013 and references therein). Two thousand year-SST and -salinity records from the Makassar Strait (Oppo et al., 2009) also support a strong link between Pacific Ocean climate and the AM. However, comparison of SST histories in the South China Sea and eastern equatorial Pacific SST suggests an El Niño-like condition for the last glacial time (Koutavas et al., 2002), opposite to the findings by Lea et al. (2000). The study by Koutavas et al. (2002) does not support our argument at MIS 6.5.*

Sea level change could be one of the secondary factors. Marine proxy records and model simulations show that the exposure of the Sunda shelf at the Last Glacial Maximum (LGM) associated with a low sea-level condition can alters regional hydrologic pattern in Southeast Asia (DiNezio and Tierney, 2013). During the LGM, the strong Pacific equatorial SST gradient could strengthen the Pacific Walker circulation and increase rainfall in the west tropical Pacific. While, as pointed out by DiNezio and Tierney (2013), both of the proxies and model simulations are highly uncertain renditions to climate history, multi-proxy records and high precise models are critical to understand paleoclimate.”. (Lines 250-268)

R2.5: The discussion of the Dole effect could be shortened - it would be sufficient to state that the $\delta^{18}\text{O}_{\text{atm}}$ record from ice cores shows a strong peak at MIS 6.5 as well, and that the inferred enhanced biosphere activity fits well to enhanced precipitation in the low latitudes.

We shortened the description of Dole effect and **deleted** the following sentences: “The Dole effect was first described by Dole in 1936. This effect is an inequality of $\delta^{18}\text{O}$ values between the atmosphere and seawater. Modern $\delta^{18}\text{O}$ of atmospheric O_2 ($\delta^{18}\text{O}_{\text{atm}}$) is $\sim 23.5\text{‰}$ heavier than the seawater value (Kroopnick and Craig, 1972). This inequality is caused by respiration, which prefers depleted $^{16}\text{O}_2$ rather than $^{18}\text{O}_2$, and is balanced by photosynthesis, which emits oxygen with the $\delta^{18}\text{O}$ value equal to the water used in the reaction (Guy et al., 1989), resulting in a net decrease of the $\delta^{18}\text{O}_{\text{atm}}$ value. Accordingly, the $\delta^{18}\text{O}_{\text{atm}}$ variation can depend on the activity of photosynthesis.”.

R2.6: Detailed comments:

R2.6.1: The authors should consider shortening the title.

We shortened the title from “Variability of the Asian summer monsoon during the penultimate glacial/interglacial period inferred from stalagmite oxygen isotope records from Yangkou cave, Chongqing, southwestern China” to “*Stalagmite-inferred variability of the Asian summer monsoon during the penultimate glacial/interglacial period*”.

R2.6.2: Abstract:

L. 5 “mainly from Sanbao”: What about the Hulu and Dongge records (which are further apart from Sanbao than the record presented here)? I assume the authors mean that only Sanbao provides a continuous, long record, but the current statement neglects the other available records.

Thank this reviewer for giving this comment. We revised the sentence to “*However, this long-term continuous ASM variability is inferred primarily from oxygen isotope records of stalagmites, mainly from Sanbao cave in mainland China, and may not provide a comprehensive picture of ASM evolution.*” (Lines 31-33)

R2.6.3: Introduction:

Page 6289

L. 22-25: Records from other archives besides speleothems should be mentioned here, like the Loess sequences or lake records.

We accepted the suggestion given by this reviewer and added Loess records in the reference. We wrote “Recent studies have led to significant advances in understanding Quaternary ASM evolution on different time scales (e.g., An, 2000; Wang et al., 2001; 2008; Fleitmann et al., 2003; 2004; *Rousseau et al. 2009*; Cheng et al., 2009; 2012b; Zhang et al., 2008; Sinha et al., 2011).” (Lines 55-58)

R2.6.4: Page 6290

L. 20-23: This sentence again disregards the replication already achieved by other speleothem records (such as that from Hulu cave shown in Figure 5).

Thank this reviewer for pointing out this point. We revised the sentence to “Comparison with records from other Chinese caves (Cheng et al., 2006; 2009; Wang et al., 2008) confirms the fidelity of Sanbao cave-inferred ASM intensities.”. (Lines 79-81) Hulu and Sanbao records were studied in the cited references.

R2.6.5: Material and Methods:

Dating: Since the dating uses three different isotopes of U and Th, the authors should either say “ ^{238}U - ^{234}U - ^{230}Th dating” or simply U-Th dating. The authors should mention here details currently only given in the footnotes to Table 1, namely, which half-lives were used and the assumed detrital Th isotope ratio. It is furthermore not clear what is included in the errors. E.g., is the uncertainty of the detrital Th ratio included?

We replaced all “ ^{230}Th dating” by “U-Th dating” throughout the manuscript. The details about the decay constants, assumed detrital Th isotope ratio and error calculation were added.

We wrote “The decay constants used are $9.1577 \times 10^{-6} \text{ yr}^{-1}$ for ^{230}Th and $2.8263 \times 10^{-6} \text{ yr}^{-1}$ for ^{234}U (Cheng et al., 2000), and $1.55125 \times 10^{-10} \text{ yr}^{-1}$ for ^{238}U (Jaffey et al., 1971). All errors of U-Th isotopic data and U-Th dates are two standard deviations (2σ) unless otherwise noted. Age (before AD 1950) corrections were made using an $^{230}\text{Th}/^{232}\text{Th}$ atomic ratio of $4 \pm 2 \text{ ppm}$, which are the values for material at secular equilibrium, with the crustal $^{232}\text{Th}/^{238}\text{U}$ value of 3.8 (Taylor and McLennan, 1995) and an arbitrary uncertainty of 50%.” (Lines 104-111)

R2.7: Minor comments

R2.7.1:

Page 6289

L. 2-4: give references

Thank this reviewer for giving this suggestion of listing references in ABSTRACT. However, for this journal, references should not be cited. One of online guidelines is “Reference citations should not be included in this section,...”. So, we cannot give references here. Besides, listing the related references is not urgently required here.

R2.7.2:

L. 9: time series supports the strong

Corrected.

R2.7.3:

L. 15: past five G/IG cycles

Corrected. It was a typo. We corrected “fiver” to “five”.

R2.7.4: Page 6291

L. 11: Use the same ages for start and end of the record as in the rest of the manuscript.

Corrected. We corrected the ages for start and end of our record, such as 124-206 kyr BP, throughout the manuscript.

R2.7.5: L. 16: 53 instead of fifty-three

Arabic numerals cannot be the 1st word in a sentence. We still wrote “*Fifty three powdered subsamples, 60-80 mg each, were drilled from the polished surface along the deposit lamina of the five stalagmites (Fig. 2, Table 1), on a class-100 bench in a class-10,000 subsampling room.*”. (Lines 97-100)

R2.7.6: Page 6292

L. 17: 100s - 10000 ppt

Corrected.

R2.7.7: L. 21: One to two

Corrected.

R2.7.8: Page 6293

L. 17-19: leave out the exact time intervals for $\delta^{18}\text{O}$ maxima and minima; these can be seen in the Figure. Replace “_” by “to”

Corrected. We deleted the time intervals. We changed this sentence from “This $\delta^{18}\text{O}$ record varies from -10‰ ~ -9‰ at 124-127, 141-155, 165-177, and 193-201 kyr BP, to -7‰ ~ -6‰ at 128-136, 155-165, 177-190, and 201-206 kry BP.” to “*This $\delta^{18}\text{O}$ record varies from -10‰ to -4‰.*”. (Lines 151-152)

R2.7.9: Page 6294

L. 20: “ thermal conditions” is a vague expression

Corrected. We revised it to “...NH insolation...” (Line 181)

R2.7.10: Page 6297

L. 7: encompassed instead of enclosed

Corrected.

R2.7.11: Table 1: Ages are in kyr (not yr). Also, the Th isotope ratio for date YK5-08 contains too many digits.

Corrected. Thank this reviewer for this comment. We corrected the “yr” to “kyr” and shortened the digits of the isotope ratio for date YK5-08. Please refer to the revised Table 1 for details.

R2.7.12: Figure 1: The colored arrow for the trade winds is confusing.

In order to avoid the confusion, we changed the color of the arrow for the trade winds to only blue color shown below.

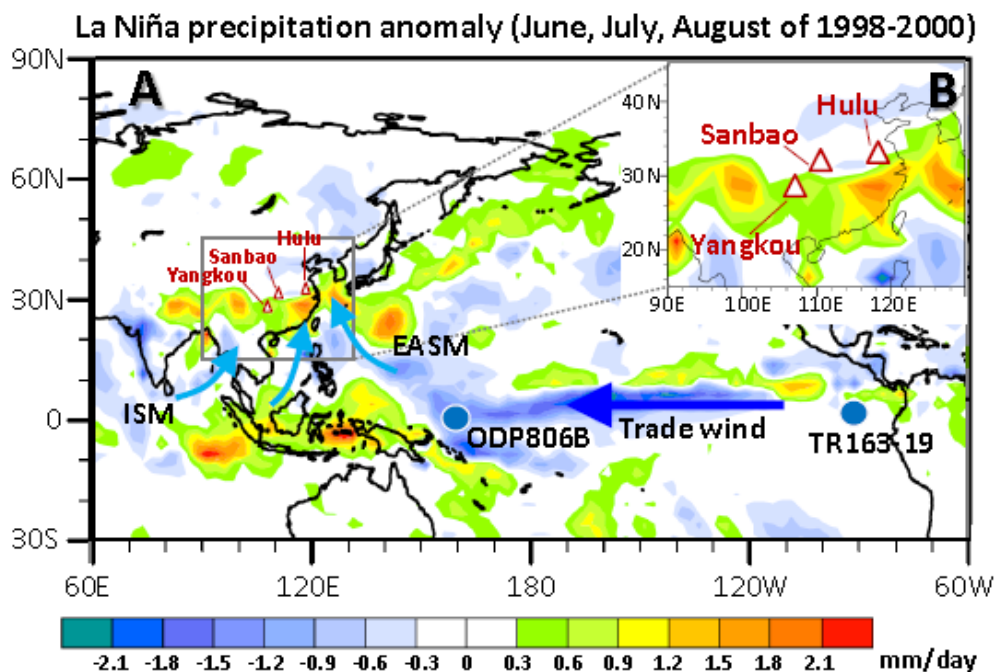


Figure R1. Revised figure 1.

References:

Cai, Y. J., Cheng, H., An, Z., Edwards, R. L., Wang, X., Tan, L., and Wang, J.: Large variations of oxygen isotopes in precipitation over south-central Tibet during Marine Isotope Stage 5, *Geology*, 38, 243-246, 2010a.

Cheng, H., Sinha, A., Wang, X., Cruz, F. W., and Edwards, R. L. (2012), The global paleomonsoon as seen through speleothem records from Asia to the Americas, *Clim. Dynam.*, 39, 1045–1062.

DiNezio, P. N., & Tierney, J. E.: The effect of sea level on glacial Indo-Pacific climate, *Nature Geosci.*, 6(6), 485-491, 2013.

Koutavas, A., Lynch-Stieglitz, J., Marchitto, T. M., and Sachs, J. P.: El Niño-like pattern in ice age tropical Pacific sea surface temperature, *Science*, 297, 226–230, 2002.

Lea, D. W., Pak, D. K., and Spero, H. J.: Climate impact of late Quaternary equatorial Pacific sea surface temperature variations, *Science*, 289, 1719-1724, 2000.

Masson, V., Braconnot, P., Cheddadi, R., Jouzel, J., Marchal, O., and de Noblet, N.: Simulation of intense monsoons under glacial conditions, *Geophys. Res. Lett.*, 27, 1747–1750, 2000.

Rousseau, D. D., Wu, N., Pei, Y., Li, F.: Three exceptionally strong East-Asian summer monsoon events during glacial times in the past 470 kyr. *Clim. Past*, 5, 157-169, 2009.

Sun, Y., Clemens, S. C., Morrill, C., Lin, X., Wang, X., and An, Z.: Influence of Atlantic meridional overturning circulation on the East Asian winter monsoon, *Nature Geosci.*, 5(1), 46-49, 2012.

Taylor, S. R., and McLennan, S. M.: The geochemical evolution of the continental crust. *Rev. Geophys.* 33, 241-265, 1995.

Ziegler, M., Tuenter, E., Lourens, L. J.: The precession phase of the boreal summer monsoon as viewed from the eastern Mediterranean (ODP Site 968). *Quaternary Sci. Rev.*, 29, 481-1490, 2010.